

## Cooperative Reductive Elimination: The Missing Piece in the Oxidative-Coupling Mechanistic Puzzle

Ignacio Funes-Ardoiz and Feliu Maseras\*

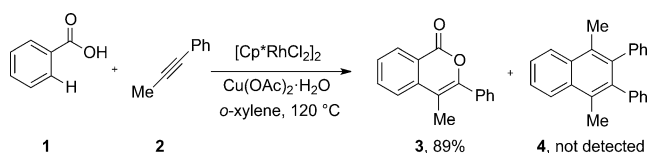
**Abstract:** The reaction between benzoic acid and methylphenylacetylene to form an isocoumarin is catalyzed by  $\text{Cp}^*\text{Rh}(\text{OAc})_2$  in the presence of  $\text{Cu}(\text{OAc})_2(\text{H}_2\text{O})$  as an oxidant and a leading example of oxidative-coupling reactions. Its mechanism was elucidated by DFT calculations with the B97D functional. The conventional mechanism, with separate reductive-elimination and reoxidation steps, was found to yield a naphthalene derivative as the major product by  $\text{CO}_2$  extrusion, contradicting experimental observations. The experimental result was reproduced by an alternative mechanism with a lower barrier: In this case, the copper acetate oxidant plays a key role in the reductive-elimination step, which takes place through a transition state containing both rhodium and copper centers. This cooperative reductive-elimination step would not be accessible with a generic oxidant, which, again, is in agreement with available experimental data.

Direct catalytic C–H activation is an appealing option for the synthesis of complex organic molecules.<sup>[1]</sup> In contrast to the widely applied cross-couplings,<sup>[2,3]</sup> it does not require the placement of a halide or any other leaving group in the position to be activated, and it improves atom economy by reducing the formation of waste products. When combined with the facile activation of an acidic O–H or N–H bond in the same molecule, direct C–H activation opens the way to annulative coupling processes with great potential.<sup>[4]</sup> However, the common need for an external oxidant has hindered the further development of such processes. If the two hydrogen atoms depart as protons, as is normally the case, the catalytic system will gain two electrons, which then have to be removed prior to a new catalytic cycle. Oxidative-coupling processes catalyzed by transition-metal complexes based on palladium,<sup>[4a,5]</sup> rhodium,<sup>[6]</sup> ruthenium,<sup>[4b,7]</sup> and copper<sup>[8]</sup> have been reported, but the issue of the oxidant remains challenging.

Such reactions only seem to be efficient with certain combinations of catalyst and oxidant. For instance, in reactions with the  $\text{Rh}^{\text{III}}/\text{Rh}^{\text{I}}$  redox pair as the catalyst, the

oxidant of choice is usually the  $\text{Cu}^{\text{II}}$  species  $\text{Cu}(\text{OAc})_2 \cdot \text{H}_2\text{O}$ , which is reduced to a  $\text{Cu}^{\text{I}}$  complex during the reaction.<sup>[9–11]</sup> The copper salt has been postulated to play an active role,<sup>[11]</sup> but detailed mechanistic evidence is scarce. Jones and co-workers showed by UV/Vis monitoring that a Rh diacetate species is formed in the presence of high acetate concentrations.<sup>[12]</sup> The presence of additional acetate, introduced as NaOAc, was also shown to be critical for the isolation of intermediates in the oxidative coupling of isoquinolones with alkynes.<sup>[13]</sup> The oxidant role of the copper center was not examined in detail in either of these experimental studies or in the computational analyses<sup>[14]</sup> that have been carried out on related processes with  $\text{Rh}^{\text{III}}/\text{Cu}^{\text{II}}$  systems. Herein, we computationally examine the specific role of  $\text{Cu}^{\text{II}}$  in the mechanism of this process.

For our study, we chose one of the leading examples of this type of chemistry, an oxidative coupling reported by Miura, Satoh, and Ueura, which is shown in Scheme 1.<sup>[9]</sup> We were particularly interested in the effect of the oxidant on the selectivity of the reaction.<sup>[9b]</sup> When copper diacetate is used as the oxidant, isocoumarin **3** is formed in high yield. In contrast, when other oxidants, such as  $\text{AgOAc}$ , are used,  $\text{CO}_2$  extrusion takes place, resulting in naphthalene derivative **4** as the major



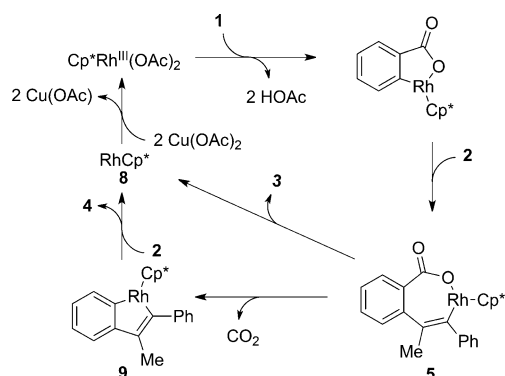
**Scheme 1.** Reported oxidative coupling between benzoic acid and an alkyne.<sup>[9]</sup>

product. We studied the key steps in this process through geometry optimizations in *ortho*-xylene solution with the B97D functional. The only simplification from the real system consisted in replacing  $\text{Cp}^*$  by  $\text{Cp}$ . A functional calibration showed that the results were similar to those obtained with M06-D3, B3LYP-D3, BP86-D3, and  $\omega\text{B97x-D}$ . Inclusion of dispersion was found to be critical (see the Supporting Information for full computational details and information on functional and basis set calibration).

The starting point for our mechanistic study was the proposal put forward by Miura, Satoh, and Ueura, which is summarized in Scheme 2. The reaction is initiated by protonation and displacement of one of the acetate ligands in the catalyst by benzoic acid. The second acetate participates in a concerted metalation deprotonation (CMD) step, which leads to cleavage of the *ortho* C–H bond.<sup>[15]</sup> Insertion of an

[\*] I. Funes-Ardoiz, Prof. F. Maseras  
Institute of Chemical Research of Catalonia (ICIQ)  
The Barcelona Institute of Science and Technology  
Avgda. Països Catalans, 16, Tarragona (43007), Catalonia (Spain)  
E-mail: fmaseras@iciq.es  
Prof. F. Maseras  
Department de Química  
Universitat Autònoma de Barcelona  
Bellaterra (08193), Catalonia (Spain)

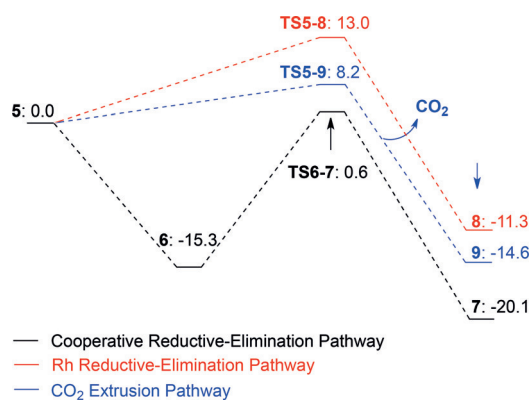
Supporting information and ORCID(s) from the author(s) for this article are available on the WWW under <http://dx.doi.org/10.1002/anie.201510540>.



Scheme 2. Original mechanistic proposal.<sup>[9b]</sup>

alkyne into the Rh–C bond then leads to intermediate **5**, which contains a seven-membered cyclometalated ring. All of these steps leading up to intermediate **5** have been well characterized for related systems as having low barriers. This hypothesis was confirmed for this system by calculations that are shown in the Supporting Information.

Intermediate **5** can evolve through one of the two alternative paths depicted in Scheme 2 to yield one of the two possible products, **3** or **4**, and to regenerate the catalyst. We computationally studied the reactivity of **5** and found, to our surprise, that the path leading to CO<sub>2</sub> extrusion is clearly favored, as shown in the free-energy profiles in Scheme 3. The direct reductive-elimination pathway through **TS5-8**, with geometrical features usually associated with these processes,<sup>[16]</sup> has a free-energy barrier of 13.0 kcal mol<sup>−1</sup> relative to **5**.



Scheme 3. Free-energy profile of the selectivity-determining step of the reaction. All energies are given in kcal mol<sup>−1</sup> relative to intermediate **5**.

The value is modest, but clearly higher than that for CO<sub>2</sub> extrusion through **TS5-9**, which is 8.2 kcal mol<sup>−1</sup> relative to **5**. We analyzed possible alternative paths that involve the coordination of acetic acid in the reaction medium, but the barrier for reductive elimination was even higher (26.5 kcal mol<sup>−1</sup>; see the Supporting Information, Figure S3).

As intermediate **5** prefers to evolve towards CO<sub>2</sub> extrusion, which contradicts the experimental observation, we decided to examine the possibility of the Cu<sup>II</sup> reducing agent interacting directly with **5**. This was not trivial, as Cu-

(OAc)<sub>2</sub>·H<sub>2</sub>O does not exist primarily as a monometallic complex in solution. It is mainly found in a dimetallic state, with the additional complication that the acetate ligand may exchange with other ligands, such as chloride (from the Cp<sup>\*</sup>RhCl<sub>2</sub> catalyst precursor), that are also available in the reaction mixture. We found that both [Cu(OAc)<sub>2</sub>(H<sub>2</sub>O)]<sub>2</sub> and [CuCl(OAc)(H<sub>2</sub>O)]<sub>2</sub> form stable adducts with intermediate **5**. The second one of these adducts, with the chlorinated copper species, leads to the productive pathway for reductive elimination indicated in Scheme 3, with the highest free-energy point of **TS6-7** being only 0.6 kcal mol<sup>−1</sup> in energy relative to **5**. This is much lower than the energy of the transition state of the alternative CO<sub>2</sub> extrusion pathway.

Figure 1 shows the structure of the key transition state **TS6-7** in this favored pathway. In this transition state, as well as in the related intermediates **6** and **7** (see the Supporting Information), there is a direct interaction between one of the carboxylate oxygen atoms and one of the copper centers,

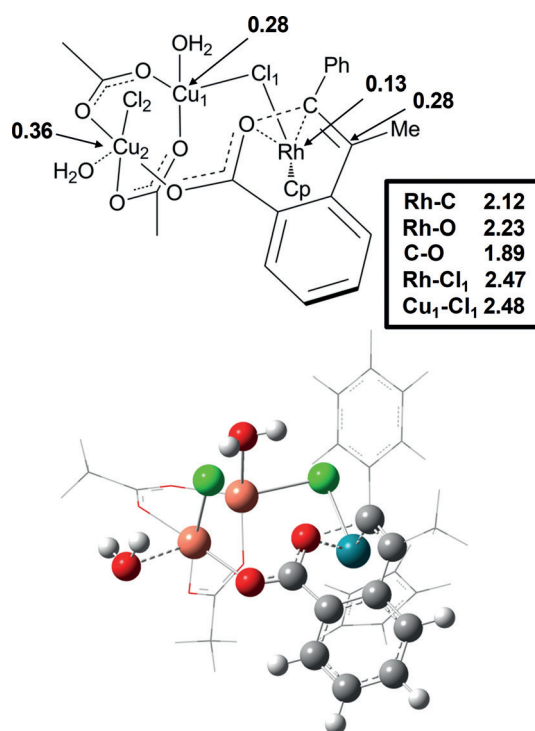
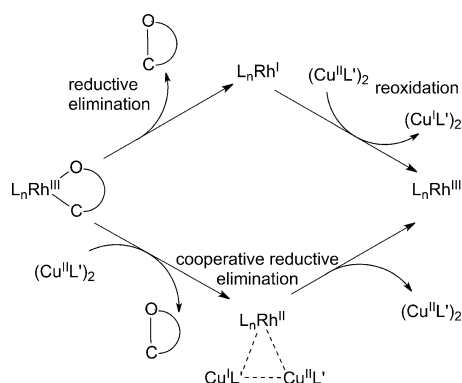


Figure 1. Key transition state (**TS6-7**) of the cooperative reductive-elimination pathway with spin densities and bond lengths (in Å).

which hinders CO<sub>2</sub> extrusion. The structure clearly corresponds to C–O formation, as indicated by the computed normal mode associated with the imaginary frequency and the C–O bond distance of 1.89 Å. The bridging position of the chlorine atom between Cu and Rh, with M–Cl distances of 2.47 and 2.48 Å, respectively, is also noteworthy. This bridge stabilizes the adduct and favors electron transfer between the metal centers.

Figure 1 also reports the spin densities, which provide information on the underlying features of this step. Two unpaired electrons are present because each initial Cu<sup>II</sup> center contains one unpaired electron, and our calculations indicate

that the dimer is most stable in a triplet spin state, as expected. The triplet lies  $0.1 \text{ kcal mol}^{-1}$  in energy below the open-shell singlet and  $6.2 \text{ kcal mol}^{-1}$  below the closed-shell singlet. The ground state for species **6**, **TS6–7**, and **7** is a triplet. The open-shell singlet state for the key species **TS6–7** is  $1.1 \text{ kcal mol}^{-1}$  above the triplet state with a qualitatively similar spin distribution and thus not discussed here. Concerning the triplet ground state, Figure 1 indicates the presence of significant spin density on rhodium (0.13) and one of the carbon atoms coming from the alkyne (0.28). Remarkably, the spin density on the two copper centers is only mildly higher (0.28, 0.36). The presence of spin density on the rhodium moiety of the adduct strongly suggests that the  $\text{Rh}^{\text{III}}/\text{Rh}^{\text{I}}$  description is not appropriate for the process taking place, as both of these oxidation states are associated with closed-shell distributions. Instead, we favor a scenario where  $\text{Rh}^{\text{III}}$  is partially reduced to  $\text{Rh}^{\text{II}}$ , and the other electron is transferred directly to the dicopper unit, with one  $\text{Cu}^{\text{II}}$  and one  $\text{Cu}^{\text{I}}$  center. A similar scenario would be obtained with the open-shell singlet spin state, but at a slightly higher energy (see the Supporting Information). This process therefore is an unusual reductive elimination, as summarized in Scheme 4. Only one of the two electrons from the anionic organic ligands goes to the adjacent metal center, while the other one is transferred directly to the final oxidant. We thus refer to this process as cooperative reductive elimination (CRE).



**Scheme 4.** Differences between the conventional mechanism (reductive elimination followed by reoxidation, top) and the cooperative reductive-elimination mechanism (bottom).

The spin densities in **6** and **7** (Figure S4) confirm the validity of this scenario. The total spin density on the two Cu centers decreases from 0.81 to 0.57 upon going from **6** to **7**, whereas the density at Rh increases from 0.14 to 0.59. One of the semi-occupied molecular orbitals in **TS6–7** is also mostly located on the Rh moiety of the system (Figure S5), corroborating the CRE proposal. After reductive elimination, the trimetallic complex **7** reorganizes; the organic product **3** is released (Scheme S6), and the Rh center then transfers one electron, with assistance from the Cl bridge atoms, to regenerate the initial catalyst  $[\text{CpRhCl}_2]$  and the  $[\text{Cu}(\text{OAc})(\text{H}_2\text{O})]_2$  waste product.

It follows from the description above that this mechanism can only operate with very specific reducing agents, which

explains why oxidative coupling did not take place in the systems under study when other oxidizing agents were used instead of copper diacetate.<sup>[9]</sup> The fact that some of the acetate ligands are replaced by chloride in the active transition state also agrees with the observed influence of acetate concentration on the nature of the species present in solution.<sup>[12,13]</sup> The participation of more than one metal center in the reduction is reminiscent of the bimetallic reductive elimination observed with dinuclear  $\text{Pd}^{\text{III}}$  complexes,<sup>[17]</sup> but with substantial differences. The role of the additive is also different from that computationally determined for  $\text{AgOAc}$  and  $\text{CsF}$  in  $\text{Pd}^{\text{II}}$  C–H activation chemistry.<sup>[18]</sup>

In conclusion, we have described a new cooperative reductive-elimination mechanism that satisfactorily explains the specific role of the copper diacetate oxidant in the rhodium-catalyzed oxidative coupling of benzoic acid and alkynes. The oxidizing agent participates directly in the reductive-elimination process by taking one electron already in the reductive-elimination transition state itself. In this way, the rhodium(I) oxidation state is never reached, which constitutes a clear deviation from the commonly observed reductive-elimination pattern at transition-metal centers. We consider that this cooperative reductive-elimination mechanism may be operating in other systems where external oxidizing agents are involved. Ongoing research in our group will aim to clarify the eventual generality of this mechanism.

## Acknowledgements

Financial support from the ICIQ Foundation, MINECO (project CTQ2014-57661-R), and Severo Ochoa Excellence Accreditation 2014–2018 (SEV-2013-0319) is gratefully acknowledged. I.F.-A. acknowledges a fellowship from the ICIQ-Severo Ochoa program (SVP-2014-068662). We also thank Dr. Max García-Melchor and Dr. Nuno Bandeira for helpful discussions.

**Keywords:** C–C coupling · density functional calculations · oxidative coupling · reaction mechanisms · reductive elimination

**How to cite:** *Angew. Chem. Int. Ed.* **2016**, 55, 2764–2767  
*Angew. Chem.* **2016**, 128, 2814–2817

- [1] a) D. Alberico, M. E. Scott, M. Lautens, *Chem. Rev.* **2007**, 107, 174–238; b) L. Ackermann, R. Vicente, A. R. Kapdi, *Angew. Chem. Int. Ed.* **2009**, 48, 9792–9826; *Angew. Chem.* **2009**, 121, 9976–10011; c) J. Wencel-Delord, F. Glorius, *Nat. Chem.* **2013**, 5, 369–375.
- [2] *Metal-Catalyzed Cross-Coupling Reactions*, 2nd ed. (Eds.: A. de Meijere, F. Dieckmann), Wiley-VCH, Weinheim, **2004**.
- [3] M. García-Melchor, A. A. C. Braga, A. Lledós, G. Ujaque, F. Maseras, *Acc. Chem. Res.* **2013**, 46, 2626–2634.
- [4] a) T. Satoh, M. Miura, *Chem. Eur. J.* **2010**, 16, 11212–11222; b) L. Ackermann, *Acc. Chem. Res.* **2014**, 47, 281–295.
- [5] a) T. W. Lyons, M. S. Sanford, *Chem. Rev.* **2010**, 110, 1147–1169; b) D. C. Powers, T. Ritter, *Acc. Chem. Res.* **2012**, 45, 840–850.
- [6] a) D. A. Colby, A. S. Tsai, R. G. Bergman, J. A. Ellman, *Acc. Chem. Res.* **2012**, 45, 814–825; b) B. Ye, N. Cramer, *Acc. Chem. Res.* **2015**, 48, 1308–1318.

- [7] P. B. Arockiam, C. Bruneau, P. H. Dixneuf, *Chem. Rev.* **2012**, *112*, 5879–5918.
- [8] X.-X. Guo, D.-W. Gu, Z. Wu, W. Zhang, *Chem. Rev.* **2015**, *115*, 1622–1651.
- [9] a) K. Ueura, T. Satoh, M. Miura, *Org. Lett.* **2007**, *9*, 1407–1409; b) K. Ueura, T. Satoh, M. Miura, *J. Org. Chem.* **2007**, *72*, 5362–5367.
- [10] a) D. R. Stuart, M. Bertrand-Laperle, K. M. N. Burgess, K. Fagnou, *J. Am. Chem. Soc.* **2008**, *130*, 16474–16475; b) T. K. Hyster, T. Rovis, *J. Am. Chem. Soc.* **2010**, *132*, 10565–10569; c) L. Huang, Q. Wang, J. Qi, X. Wu, K. Huang, H. Jiang, *Chem. Sci.* **2013**, *4*, 2665–2669; d) J. Shi, Y. Yan, L. Qiu, H. E. Xu, W. Yi, *Chem. Commun.* **2014**, *50*, 6483–6486; e) J. Zheng, S.-B. Wang, C. Zheng, S. L. You, *J. Am. Chem. Soc.* **2015**, *137*, 4880–4883; f) R. B. Dateer, S. Chang, *J. Am. Chem. Soc.* **2015**, *137*, 4908–4911; g) A. M. Martínez, J. Echavarren, I. Alonso, N. Rodríguez, R. Gómez-Arrayás, J. C. Carretero, *Chem. Sci.* **2015**, *6*, 5802–5814.
- [11] a) L. Li, W. W. Brennessel, W. D. Jones, *J. Am. Chem. Soc.* **2008**, *130*, 12414–12419; b) F. W. Patureau, J. Wencel-Delord, F. Glorius, *Aldrichimica Acta* **2012**, *45*, 31–41.
- [12] L. Li, W. W. Brennessel, W. D. Jones, *Organometallics* **2009**, *28*, 3492–3500.
- [13] N. Wang, B. Li, H. Song, S. Xu, B. Wang, *Chem. Eur. J.* **2013**, *19*, 358–364.
- [14] a) L. Xu, Q. Zhu, G. Huang, B. Cheng, Y. Xia, *J. Org. Chem.* **2012**, *77*, 3017–3024; b) N. Quiñones, A. Seoane, R. García-Fandiño, J. L. Mascareñas, M. Gulías, *Chem. Sci.* **2013**, *4*, 2874–2879; c) D. L. Davies, C. E. Ellul, S. A. Macgregor, C. L. McMullin, *J. Am. Chem. Soc.* **2015**, *137*, 9659–9669; d) J. Jiang, R. Ramozzi, K. Morokuma, *Chem. Eur. J.* **2015**, *21*, 11158–11164.
- [15] a) D. L. Davies, S. M. A. Donald, O. Al-Duaij, S. A. Macgregor, M. Pölleth, *J. Am. Chem. Soc.* **2006**, *128*, 4210–4211; b) D. García-Cuadrado, P. de Mendoza, A. A. C. Braga, F. Maseras, A. M. Echavarren, *J. Am. Chem. Soc.* **2007**, *129*, 6880–6886; c) S. I. Gorelsky, D. Lapointe, K. Fagnou, *J. Am. Chem. Soc.* **2008**, *130*, 10848–10849.
- [16] a) V. P. Ananikov, D. G. Musaev, K. Morokuma, *J. Am. Chem. Soc.* **2002**, *124*, 2839–2852; b) M. Pérez-Rodríguez, A. A. C. Braga, M. Garcia-Melchor, M. H. Pérez-Temprano, J. A. Casares, G. Ujaque, A. R. de Lera, R. Álvarez, F. Maseras, P. Espinet, *J. Am. Chem. Soc.* **2009**, *131*, 3650–3657.
- [17] D. C. Powers, D. Benitez, E. Tkatchouk, W. A. Goddard III, T. J. Ritter, *J. Am. Chem. Soc.* **2010**, *132*, 14092–14103.
- [18] M. Anand, R. B. Sunoj, H. F. Schaefer, *J. Am. Chem. Soc.* **2014**, *136*, 5535–5538.

Received: November 13, 2015

Revised: December 22, 2015

Published online: January 25, 2016